Development 139, 2926-2934 (2012) doi:10.1242/dev.082396

Identification of a novel developmental mechanism in the generation of mesothelia

Nichelle I. Winters[1], Rebecca T. Thomason[1] and David M. Bader[1,2,*]

SUMMARY

Mesothelium is the surface layer of all coelomic organs and is crucial for the generation of their vasculature. Still, our understanding of the genesis of this essential cell type is restricted to the heart where a localized exogenous population of cells, the proepicardium, migrates to and envelops the myocardium supplying mesothelial, vascular and stromal cell lineages. Currently it is not known whether this pattern of development is specific to the heart or applies broadly to other coelomic organs. Using two independent long-term lineage-tracing studies, we demonstrate that mesothelial progenitors of the intestine are intrinsic to the gut tube anlage. Furthermore, a novel chick-quail chimera model of gut morphogenesis reveals these mesothelial progenitors are broadly distributed throughout the gut primordium and are not derived from a localized and exogenous proepicardium-like source of cells. These data demonstrate an intrinsic origin of mesothelial cells to a coelomic organ and provide a novel mechanism for the generation of mesothelial cells.

KEY WORDS: Mesothelium, Splanchnic mesoderm, Intestine, Chick, Quail

INTRODUCTION

The vertebrate coelom, or body cavity, and internal organs housed therein are all lined by a simple squamous epithelium called mesothelium. In the healthy adult, mesothelia are relatively quiescent – their primary function is to form a non-adhesive surface for the movement of organs (Mutsaers and Wilkosz, 2007). However, mesothelia are also recognized as crucial players in peritoneal sclerosis (Chegini, 2008; Yung and Chan, 2009), in the regulation of the injury microenvironment in myocardial infarction (Zhou et al., 2011) and for their ability to promote revascularization of diverse tissues, including the heart (Takaba et al., 2006; Zhang et al., 1997). These functions of mesothelium in injury and repair reflect the dynamic behavior of mesothelia in embryonic development. Although mesothelia are universally distributed in the pericardial, pleural and peritoneal cavities of all vertebrates, our understanding of mesothelial development is largely restricted to one organ: the heart.

Ho, Shimada and Manasek demonstrated that cardiac mesothelium (epicardium) originated from a discrete population of cells termed the proepicardium (PE) localized outside of the initial heart tube (Ho and Shimada, 1978; Manasek, 1969). Originating from the region of the sinus venosus, these cells migrate as an epithelium across the pericardial space to contact the naked myocardium (Ishii et al., 2010). Further dorsal-ventral migration of this epithelium over the heart tube leads to formation of the epicardium. Thus, epicardial precursors do not arise in situ but are recruited from a localized cell source exogenous to the splanchnic mesoderm of the developing organ.

Subsequent lineage-tracing studies revealed that specific cells within the epicardium undergo epithelial-mesenchymal transition (Wu et al., 2010), invade the myocardium and differentiate into fibroblasts, vascular smooth muscle and endothelial cell populations (Dettman et al., 1998; Mikawa and Gourdie, 1996). Hepatic, pulmonary and intestinal mesothelia have since been shown to provide vasculogenic and stromal populations to their respective organs (Asahina et al., 2011; Eralp et al., 2005; Morimoto et al., 2010; Pérez-Pomares et al., 2004; Que et al., 2008; Wilm et al., 2005).

Wilm et al. (Wilm et al., 2005) demonstrated that the mesothelial marker Wilms' tumor protein 1 (Wt1) first appeared in the mesentery of the intestine and then later encompassed the gut tube in a dorsal-ventral direction. This expression pattern mirrored the dorsal-ventral migration of the epicardium seen in the heart and, from these data, our group hypothesized that 'non-resident cells migrate to and over the gut to form the serosal mesothelium' (Wilm et al., 2005). These data, in conjunction with the shared vasculogenic potential of mesothelia, suggested that the mechanism of mesothelial development and the function of this cell type in embryogenesis may be conserved in diverse coelomic cavities.

In contrast to the extensive analysis of epicardial development, careful examination of the primary literature reveals that little, if anything, is known about the origin of mesothelial cells in any coelomic organ other than the heart. Additionally, a change in terminology contributes to confusion in the literature regarding this cell type. The term 'mesothelium' originally referred to the entire epithelial component of mesoderm as differentiated from the loose mesenchyme (Minot, 1890). The term did not refer to the specific simple squamous cell type we currently identify as mesothelium. Still, a review authored by Minot (Minot, 1890) using this original terminology appears to form the basis for the modern description on the origin of vertebrate coelomic mesothelia (Moore and Persaud, 1998; Mutsaers, 2002). An extensive review of the literature reveals no primary data addressing the origin of mesothelium. Taken together, it is clear that the program of proepicardial/epicardial development stands alone as a definitive model of development of this widely distributed cell type that is so crucial for vertebrate organogenesis.

A question arises: is there a common mechanism of mesothelial development? Fundamental to answering this question is determining the origin of mesothelial precursors in diverse

[1]Department of Cell and Developmental Biology, Vanderbilt University, Nashville, TN 37232, USA. [2]Department of Medicine, Vanderbilt University, Nashville, TN 37232, USA.

*Author for correspondence (david.bader@vanderbilt.edu)

Accepted 22 May 2012

coelomic organs. Thus, we examined intestinal development to determine whether mesothelium originated from an exogenous localized source, as seen in the heart, or, conversely, from a resident population of mesothelial progenitors within the gut itself. Using three independent experimental models, we demonstrate that the intestine derives its mesothelial layer from progenitor cells broadly resident within the splanchnic mesoderm and not from a PE-like structure extrinsic to the developing organ. These data provide new information concerning a fundamental process of intestinal development and reveal diversity in mechanisms that regulate the generation of mesothelia.

MATERIALS AND METHODS

In situ hybridization

In situ hybridization was performed according to standard protocols (McGlinn and Mansfield, 2011). The *Wt1* template (GenBank Accession Number AB033634.1) was kindly provided by Dr Jorg Manner (Georg-August University of Gottingen, Germany) (Schulte et al., 2007).

Immunohistochemistry and co-localization analysis

Immunohistochemical analysis of sectioned chick (*Gallus gallus*) or quail (*Coturnix japonica*) embryos was as published previously (Osler and Bader, 2004). All animal procedures were performed in accordance with institutional guidelines and IACUC approval. Chick embryos were staged according to Hamburger and Hamilton (Hamburger and Hamilton, 1992). The following primary antibodies were used: anti-GFP (Invitrogen A11122, 1:200); anti-laminin (Abcam Ab11575, 1:50); anti-laminin (DSHB 31 or 31-2, 1:25); anti-neurofilaments (DSHB RT97, 1:50); anti-smooth muscle actin (Sigma A2547, 1:200); anti-smooth muscle actin (Abcam Ab5694, 1:200); QCPN (DSHB undiluted); 8F3 (DSHB, 1:25); anti-PGP9.5 (Zymed 38-1000, 1:200); anti-cytokeratin (Abcam Ab9377, 1:100); and QH1 (DSHB, 1:200). The following secondary antibodies were used at a 1:500 dilution: Alexa Fluor 488 or 568 goat anti-rabbit (Invitrogen); and Alexa Fluor 488 or 568 goat anti-mouse (Invitrogen). TOPRO-3 (Invitrogen T3605) at 1 μmol/l was applied for 20 minutes. Sections were imaged in *z*-stacks using a LSM510 META Confocal with 0.4 μm optical slices. Each optical slice was analyzed for colocalization of the red and green channels using ImageJ followed by *z*-projection for counting of cells. All immunohistochemistry images presented in figures are *z*-projections.

Microinjection

Windowed chick embryos (HH14-17) were lightly stained by placing a dried strip of Neutral Red (0.2 mg/ml) in 1% agar on top of the embryo. For contrast, 0.2 μl of 10% Fast Green solution (sterile filtered) was added to 5 μl viral or pCIG suspension (7 μg/μl) and then loaded into a pulled glass needle. The agar strip was removed and ~25-30 nl were injected into both lateral cavities with aid of a micromanipulator and use of a Narishige IM300 microinjector with 2 msecond pulses at 38PSI.

Electroporation

pCIG-GFP in which GFP expression is driven by the chicken β-actin promoter was kindly provided by Dr Michael Stark (Brigham Young University, Provo, UT, USA) (Lassiter et al., 2007). Chick eggs incubated 2.5 days were windowed by withdrawing 4 ml of albumin and cutting a hole in the top of the egg shell. The vitelline membrane over the posterior region of windowed HH14-HH17 embryos was removed with a tungsten needle. After pCIG-GFP microinjection, a small hole was made outside of the vascularized region through which the positive electrode was inserted below the embryo. The negative electrode was placed on top of the embryo and five to seven, 10 msecond pulses at 15 V were delivered (ECM 830 electroporator; BTX Harvard Apparatus). After addition of Tyrode's salts solution with 1% pen/strep, the eggs were resealed with tape and incubated 8 days.

Production of pSNID retrovirus

The following plasmids were used: pSNID with both a GFP and β-gal reporter (a generous gift from Dr Jeanette Hyer, UCSF, San Francisco, CA, USA) (Venters et al., 2008); pCI-VSVG (Addgene, 1733); and pCAGGS Gag/Pol (a generous gift from Dr Connie Cepko, Harvard University, Cambridge, MA, USA). Virus was produced in Phoenix-GP cells. Pheonix-GP cells (ATCC SD-3514) were grown to 70-80% confluence in DMEM supplemented with 10% FBS and split 1:3 onto four 10 cm plates the night prior to transfection. Media was exchanged prior to transfection. For each plate, 4 μg DNA (2 μg pSNID, 1 μg VSV-G, 1 μg Gag/pol) was diluted in 100 μl serum-free DMEM. To the DNA suspension, 24 μl PEI (1 mg/ml PEI, pH 7; MW25K, Polysciences 23966-2) was added, mixed by vortexing, incubated for 15 minutes at room temperature and added to the cells overnight. Media were exchanged, collected after 24 hours, and stored at –80°C. New media were added (5 ml), collected at 48 hours, pooled with 24 hour collection, filtered (45 μmol/l) and concentrated by ultracentrifugation (SW-28 rotor, 43,000 ***g*** for 2 hours at 4°C). Supernatant was discarded and the ultracentrifuge tube drained by inverting for 60 seconds. The viral pellet was resuspended in media that remained in the ultracentrifuge tube (~50-80 μl). Polybrene (Sigma H9268) was added to the viral suspension at final concentration of 100 μg/ml. After microinjection, infected cells were detected by GFP expression in whole mount using a fluorescence-detecting microscope or in section by staining with an anti-GFP antibody.

Titer assay

D17 cells were grown to 60% confluence in six-well plates. Fresh media (DMEM + 7% FBS) with 10 μg/ml polybrene were added to the plates prior to infection. Concentrated viral suspension was serially diluted and added to the six-well plates. At 48 hours, cells were stained with X-gal to detect viral infection. The total number of positive clones in a well were counted to determine the total number of virions added. Viral titers reaching at least 10^7 virions/ml were aliquoted and stored at –80°C.

Generation of chick-quail chimeras

Splanchnopleure was dissected away from quail embryos staged 14-17. Dissection was carried out in sterile Tyrode's salt solution. Isolated splanchnopleure was bisected into anterior and posterior regions by cutting at the vitelline artery and then anterior and posterior splanchnopleure was further subdivided into three or four pieces. Chick embryos in windowed eggs were lightly stained with a strip of neutral red in agar. The vitelline membrane was removed with a tungsten needle and a small hole made through the somatopleure over the vitelline artery. The quail splanchnopleure graft was transferred into the chick egg and pushed through the hole with forceps and a tungsten needle into the right lateral cavity. Tyrode's salt solution with 1% penicillin/steptomycin was added to replace volume and eggs were then sealed with tape and incubated for 1-14 days. The number of graft- and host-derived mesothelial cells was determined by analyzing a subset of graft-derived gut tubes at multiple levels. The mesothelial layer was distinguished by morphology combined with cytokeratin or laminin staining. Nuclei within the mesothelial layer were manually identified and then subsequently identified as either QCPN or 8F3 positive.

RESULTS

Trilaminar organization of the intestine is established prior to tube formation

The adult intestine is composed of three subdivisions or compartments: the inner mucosa with an underlying basement membrane, the middle 'mesenchymal' layers harboring stromal and visceral smooth muscle cells, and the outer mesothelium with its own basement membrane. We used immunohistochemical staining for cytokeratin, an intermediate filament expressed by epithelia, and for laminin, a component of basement membranes, to examine the intestine for establishment of these three compartments. By close examination of formation of these compartments, we sought to identify any potential mesothelial progenitor population within the gut tube either of a proepicardial-like morphology or any other tissue arrangement.

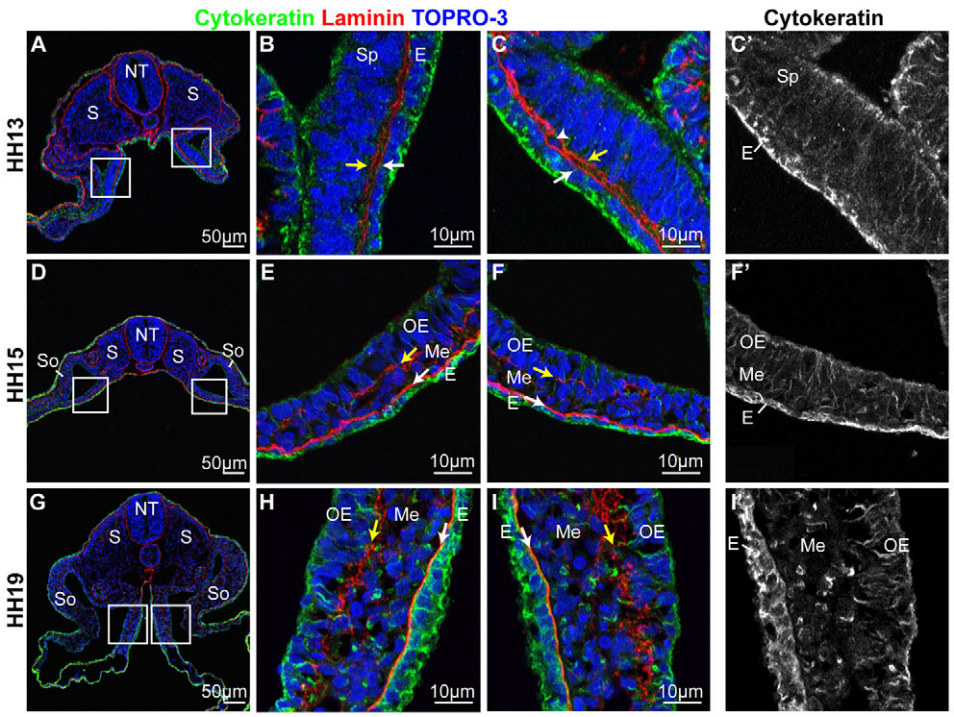

Fig. 1. A trilaminar gut tube was generated by HH15. (**A**) HH13 splanchnopleure is composed of two layers. (**B**,**C**) Boxed regions shown in A. The splanchnic mesoderm appears stratified and is underlain by a basement membrane (yellow arrow). The endoderm has its own basement membrane (white arrow). Arrowheads in C indicate a single mesenchymal cell. (**C'**) The endoderm, but not the splanchnic mesoderm, is cytokeratin positive at HH13. (**D-F**) At HH15, a mesenchymal layer resides between the aforementioned basement membranes (arrows). (**F'**) The outer epithelium is not cytokeratin positive at HH15. (**G-I**) At HH19, the mesenchymal layer has expanded (space between two arrows) and the basement membrane of the outer epithelium has fragmented (yellow arrow). (**I'**) The endoderm, but not the outer epithelium, is cytokeratin positive. E, endoderm; Me, mesenchyme; NT, neural tube; OE, outer epithelium; S, somite; So, somatic mesoderm; Sp, splanchnic mesoderm.

The splanchnopleure posterior to the heart tube of chick embryos was examined at early stages of intestinal morphogenesis, prior to gut tube closure. At the earliest stage examined, HH13, the splanchnopleure was bilaminar composed of endoderm and splanchnic mesoderm with almost no intervening mesenchymal cells (Fig. 1A-C, arrowhead). Each layer was individually underlain by a laminin-positive basement membrane that extended along the entire dorsal-ventral axis of the splanchnopleure (Fig. 1A-C, arrows).

At HH15, the splanchnopleure transitioned from having two major compartments to three. This was due to the establishment of a mesenchymal layer between the two basement membranes of the splanchnopleure (Fig. 1D-F). For ease of reference, we termed the three compartments endoderm, mesenchyme and outer epithelium though at this time the outer epithelium does not express cytokeratin (Fig. 1F′). The transition to three compartments occurred evenly throughout the splanchnopleure, and no localized PE-like structure was observed throughout the entirety of the peritoneal cavity. The outer epithelium remained stratified/pseudostratified, was underlain by a fragmented basement membrane (yellow arrow) and formed a uniform layer over the mesenchyme (Fig. 1D-F). With the appearance of the mesenchymal layer, the splanchnopleure was now in a trilaminar configuration that, as described above, is the basic organization of the adult intestine. The mesenchymal layer expanded through HH19 and the basement membrane of the outer epithelium remained fragmented (Fig. 1G-I, yellow arrow). The mesothelial marker *Wt1* was, however, not expressed specifically in the outer epithelium at these stages though *Wt1* staining was observed in the mesothelial component of the PE over the same period of time (supplementary material Fig. S1). Four days after the initial appearance of the outer epithelium (HH29, day 6) the layer attained the simple squamous morphology and robust cytokeratin expression of a definitive mesothelium (Fig. 2A-D). Thus, the three compartments of the intestine, including a potential mesothelial progenitor layer, the outer epithelium, are established very early in development prior even to intestinal tube formation.

Mesothelial progenitors are resident to the splanchnic mesoderm

As a first step in identifying the origin of mesothelial progenitors, it was necessary to determine whether the outer epithelium was derived from resident cells of the splanchnic mesoderm layer or a migratory progenitor population undetected by the analyses described above. Thus, we devised a method to label and trace cells of the splanchnic mesoderm over time. A reporter plasmid expressing green fluorescent protein (GFP) from the chick β-actin promoter was injected into the lateral cavities of HH14 chick embryos, the stage prior to establishment of the mesenchymal layer (Fig. 3A). Microinjection was followed by electroporation with the electrodes oriented directly above and below the embryo to direct the DNA ventrally into the splanchnic mesoderm.

Embryos were incubated for 6 hours post-electroporation to allow for GFP to accumulate to a detectable level and also encompass the time over which the splanchnopleure transitions from two to three layers. Whole-mount imaging of electroporated embryos revealed bilateral GFP expression restricted to the region of the lateral plate near the vitelline arteries, demonstrating the accuracy of the targeting method (Fig. 3B, arrows). Fluorescent imaging of sections through the targeted regions at 6 hours post-electroporation demonstrated that GFP-positive cells were present predominantly within the outer epithelium (71%; 454/640 total cells counted from four embryos, arrows) but also in the underlying mesenchyme (29%, 186/640 total cells counted, Fig. 3C-E, arrowheads). At no time was endoderm labeled with this method. Embryos electroporated between HH15-HH17 demonstrated similar labeling with 66% of GFP-positive cells within the outer epithelium (316/482 total cells counted; supplementary material Fig. S2). The presence of labeled cells in the outer epithelium and mesenchyme indicates the splanchnic mesoderm provides cells to both layers.

We next sought to determine whether cells of the splanchnic mesoderm later gave rise to the mesothelium. For this experiment, embryos were electroporated between HH15-HH17 and incubated

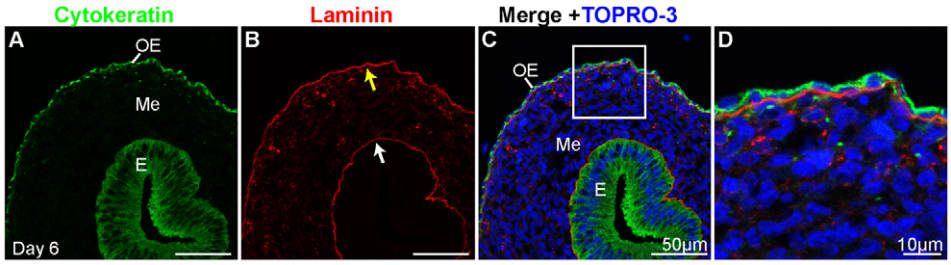

Fig. 2. Definitive intestinal mesothelium is present at HH29 (Day 6). (**A**) At day 6, a simple squamous, cytokeratin-positive (green) mesothelium is present surrounding the intestine. (**B**) A basement membrane underlies the mesothelium (red, yellow arrow). White arrow indicates endodermal basement membrance. (**C**) Merge of A and B. (**D**) Higher magnification of boxed region shown in C. E, endoderm; Me, mesenchyme; OE, outer epithelium.

for 8 days (the limit of GFP detection using this method) to day 10 of chick development. Examination of resulting small intestines revealed labeled cells were clearly resident within the mesothelial layer. These GFP-positive cells exhibited features typical of mesothelium, including a close association with the basal lamina and a squamous morphology (Fig. 4A-D, arrows). In addition to the mesothelium, GFP-positive cells were identified throughout the gut tube, including the muscularis externa (arrows) and penetrating as deep as the submucosa (Fig. 4E-H, arrowhead). Labeled cells were never observed in the endodermal mucosa. These data demonstrate that mesothelial precursors are resident to the splanchnic mesoderm and outer epithelial layer of the primitive intestine.

We used a second direct labeling approach to confirm and extend our findings. For these experiments, we used a replication-incompetent retrovirus with broad tropism and a GFP reporter gene. Incorporation of the retroviral genome into infected cells allows for long-term tracing without dilution of the label through cell division. High titer retrovirus was injected into the lateral cavities of HH14-17 embryos in the same manner as the electroporation plasmid to label the surface cells throughout the time points at which the splanchnopleure transitions between two to three compartments. Embryos were then incubated 14 days (to day 17 of development, hatching occurs at day 21) before the gut tubes were harvested.

Isolated gut tubes were first examined in whole mount for GFP expression. In embryos infected at HH14, a time prior to appearance of the middle mesenchymal layer, GFP-positive cells were present throughout the gut tube and mesentery and many appeared localized to the surface (Fig. 5A, arrows). GFP-positive cells also clearly associated with the vascular tree (Fig. 5B,B′, arrows) and distributed in deep layers (Fig. 5C, arrows).

Upon sectioning, surface GFP-positive mesothelial cells with a squamous morphology were clearly identified in close association with the external basal lamina (Fig. 6A,B, arrowhead). GFP-positive vascular smooth muscle cells were also present, consistent with previously published data (Wilm et al., 2005). Other GFP-positive, SMA-negative cells were identified peripheral to the vascular media within the adventitia (Fig. 6C,D). We did not identify any GFP-positive endothelial cells. GFP-positive cells were also identified within the submucosa and muscularis externa but not within the mucosal epithelium (Fig. 6E). Only 5% of GFP-positive cells localized within the muscularis externa were visceral smooth muscle cells [α-smooth muscle actin (SMA)-positive and spindle shaped] (Fig. 6F-H, arrowheads). The phenotype of the remaining cells could not be identified by morphology or by specific markers of smooth muscle, neurons or epithelia, and might best be characterized as stromal/mesenchymal by their location within the organ wall (Fig. 6J,L; data not shown). In embryos infected with the retrovirus between stages 15-17, after division of the splanchnic mesoderm into outer epithelium and mesenchyme, the same GFP-positive populations were identified at day 17 of development (Fig. 6I-L). This independent assay confirmed that resident splanchnic mesoderm was the origin of mesothelium and that these cells are maintained within the definitive mesothelium.

Intestinal mesothelial progenitors are localized broadly throughout the splanchnic mesoderm

The current data establish that cells resident to the splanchnic mesoderm give rise to intestinal mesothelium. We next sought to determine whether the majority of cells were derived from this

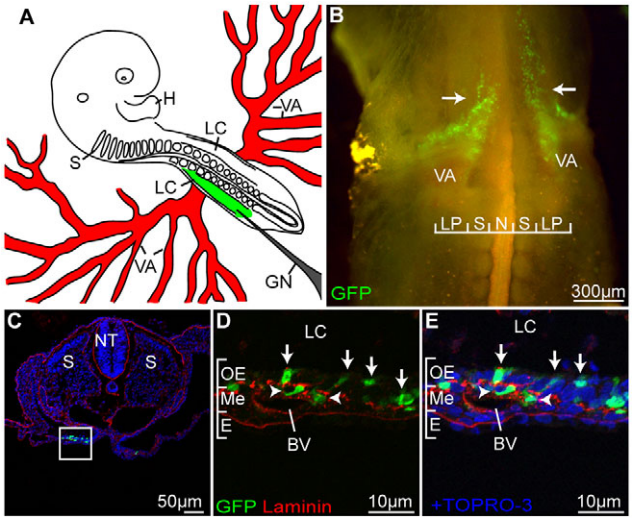

Fig. 3. Electroporation of the splanchnic mesoderm at HH14 demonstrates labeling of the outer epithelium and mesenchyme. (**A**) Schematic demonstrating injection of the GFP reporter plasmid into the right lateral cavity of an embryo in ovo. (**B**) Whole-mount image of the ventral surface of an embryo electroporated at HH14 and then incubated for 6 hours. Electrodes were placed near the vitelline artery. GFP was observed in the region near the vitelline artery and was restricted to the lateral plates (arrows). (**C**) GFP-positive cells localized to the splanchnic mesoderm. (**D**) Boxed area shown in C. GFP-positive cells were found primarily within the outer epithelium (arrows) with a few cells within the mesenchymal layer (arrowheads). No GFP-positive cells were identified in the endoderm. (**E**) Merge of D with TOPRO-3. BV, blood vessel; GN, glass needle; H, heart; LC, lateral cavity; LP, lateral plate; Me, mesenchymal layer; N, notochord; NT, neural tube; OE, outer epithelium; S, somite, VA, vitelline artery.

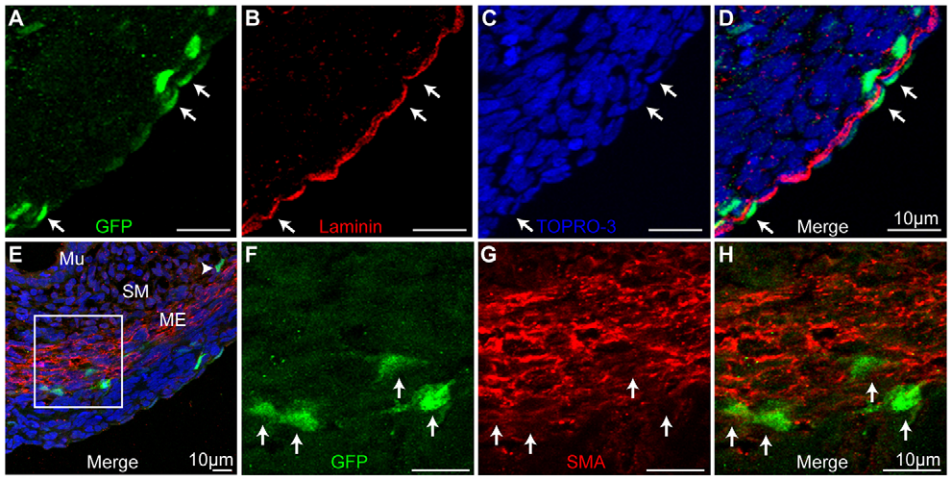

Fig. 4. DNA electroporation demonstrates that splanchnic mesoderm harbors mesothelial progenitors. Sections through gut tubes of embryos electroporated at HH15-HH17 and incubated for 8 days. (**A-D**) GFP-positive cells (arrows) were identified within the squamous mesothelial layer of the intestine associated closely with the basement membrane (laminin, red). (**E**) GFP-positive cells were also identified within the forming α-smooth muscle actin (SMA)-positive muscularis externa (boxed region) and into the submucosa (arrowhead). (**F-H**) Higher magnification of the boxed region. GFP-positive cells within the muscularis externus were not SMA positive (arrows). ME, muscularis externa; Mu, mucosa; SM, submucosa.

resident population of progenitors and whether the potential to generate mesothelium from resident cells was distributed broadly throughout the splanchnic mesoderm or restricted to subdivisions of the gut.

To address these questions, we developed a chick-quail chimera assay to analyze gut development. Bilateral splanchnopleure was isolated from HH13-17 quail embryos, divided into six or seven pieces along the AP axis, and then transplanted individually into the right lateral cavities (precursor to the coelomic cavity) of chick embryos staged between HH16 and HH18 (Fig. 7A). The host chick embryos were incubated for 14 days post-transplantation (corresponding to day 16.5 of quail development) and then harvested to identify where the transplanted tissue incorporated and whether mesothelial differentiation transpired.

Strikingly, the transplanted splanchnopleure did not incorporate into the host gut tube but rather formed an independent ‘gut tube’ within the coelomic cavity connected to the host only through a mesentery (Fig. 7B). At 14 days post-transplantation, graft-derived gut tubes were similar to a normally developing small intestine with an elongated tubular shape and a single dorsal mesentery (Fig. 7C, brackets) housing a well-organized vasculature (Fig. 7D, arrowheads; observed in 16 chick-quail chimeras). Transverse sections through graft-derived gut tubes demonstrated a remarkable intestinal organization with an inner mucosa with villus folds (arrowheads), a submucosa and a muscularis externa with smooth muscle differentiation (Fig. 7E-G). Staining for quail-specific QCPN demonstrated all layers of the graft were quail derived (Fig. 7E-G). Specific regions in the graft did not stain with QCPN but were positive for a pan-neuronal marker, PGP9.5 (supplementary material Fig. S3A-E, asterisks). Co-staining for a marker of chick cells (8F3) and PGP9.5 confirmed these cells originated from host neural crest cells (supplementary material Fig. S3F-J). Interestingly, the host-derived neural crest cells that invaded the graft organized into typical submucosal and myenteric plexuses (supplementary material Fig. S3). Transplanted splanchnopleure isolated both prior to (HH13-HH14) and after (HH15-HH17) establishment of a trilaminar configuration produced identical results (Fig. 8).

Co-staining for QCPN with cytokeratin revealed that mesothelium covering the graft-derived gut tube and within the mesentery originated from transplanted quail splanchnopleure (Fig. 8A-F, arrowheads). We quantified the number of mesothelial cells in graft-derived gut tubes that were QCPN positive and found that, on average, 85% of mesothelial cells were quail derived. Furthermore, 94% of mesothelial cells in graft-derived gut tubes

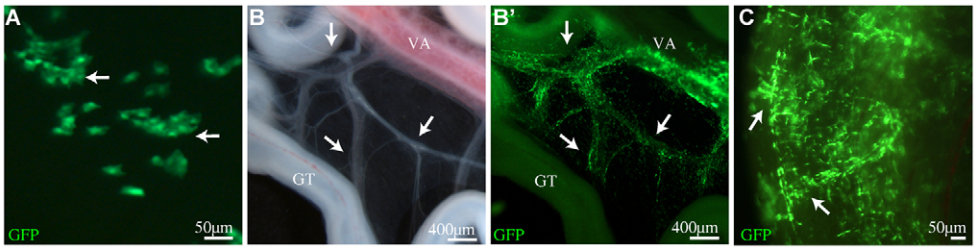

Fig. 5. Long-term retroviral lineage tracing of splanchnic mesoderm. Whole-mount images of intestine from embryos infected with virus between HH14 and HH17 and analyzed 14 days later. (**A**) High magnification of intestinal surface demonstrated cells resembling mesothelium with prominent nuclei and broad cell processes (arrows). (**B**) Bright-field image of gut tube demonstrating the vasculature (arrows). (**B′**) GFP fluorescence of gut tube pictured in B. GFP-positive cells surrounded the vasculature within the mesentery and intestine (arrows). (**C**) GFP-positive cells were also found distributed deeply in the intestine (arrows). GT, gut tube; VA, vitelline artery

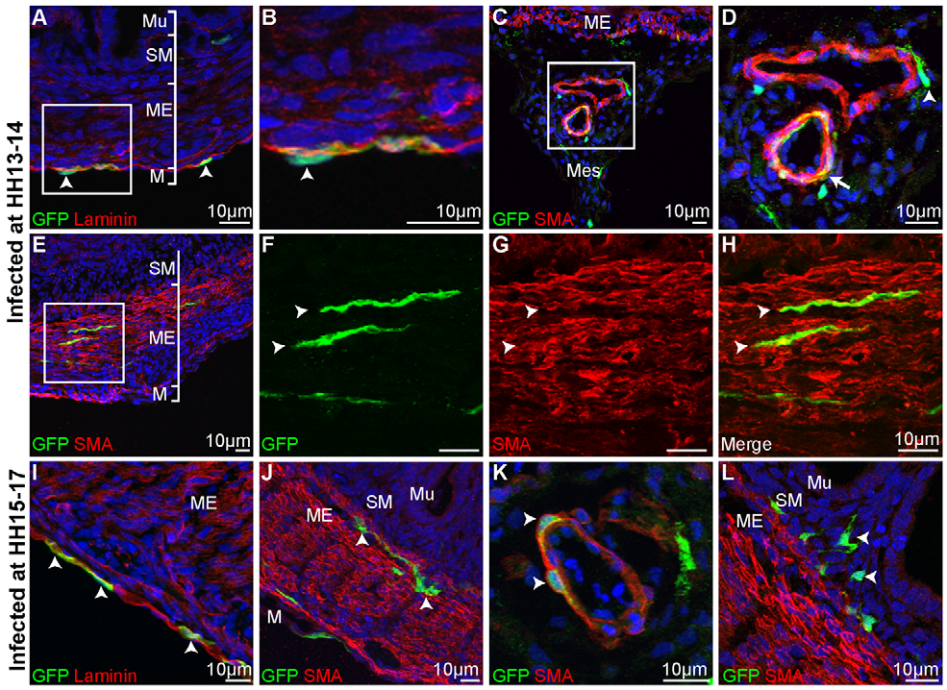

Fig. 6. Lineage tracing of splanchnic mesoderm reveals mesothelial, perivascular and mesenchymal derivatives. (A-H) Sections of intestine from embryos infected between HH13-14 and isolated 14 days later. (**A**) Squamous GFP-positive cells frequently populated the mesothelium (arrowheads) closely associating with the basement membrane (red, laminin). (**B**) High magnification of boxed area in A. (**C**) GFP-positive cells associated with large mesenteric blood vessels. (**D**) High magnification of boxed area in C demonstrates GFP-positive vascular smooth muscle cells (arrow) and perivascular cells (arrowhead). (**E**) GFP-positive cells were identified within the muscularis externa. (**F-H**) High magnification of boxed area shown in E. A rare population of GFP-positive cells found within the muscularis externus were spindle shaped and SMA positive (arrowheads). (I-L) Sections of intestine from embryos infected between HH15 and HH17, and isolated 14 days later. (**I**) Squamous GFP-positive cells populated the mesothelium (arrowheads), closely associating with the basement membrane (red, laminin). (**J**) SMA-negative mesenchymal cells within the muscularis externa layer (arrowheads). (**K**) GFP-positive vascular smooth muscle cells (arrowheads). (**L**) Submucosal GFP-positive, SMA-negative cells. M, mesothelium; ME, muscularis externus; Mes, mesentery; Mu, mucosa, SM, submucosa.

were negative for a marker specific to chick cells (8F3) (Fig. 8G-I). The difference between the two percentages is probably due to the variation in staining patterns; QCPN is a perinuclear antigen often with distinct puncta of staining, whereas 8F3 is cytoplasmic and more easily visualized (Fig. 8J-L). Both figures denote the great majority of graft-derived mesothelial cells were derived from transplanted tissue.

Tissue morphogenesis was identical between both anterior- and posterior-derived grafts and, crucial to the current studies, the mesothelium was always quail derived regardless of whether the graft was obtained from an anterior or posterior location in the source splanchnopleure (100% of cases examined, Fig. 8A-F). Taken together, these data demonstrate that mesothelial progenitors are broadly distributed along the AP axis of the intestine and there is not a localized or restricted PE-like source of mesothelial cells.

DISCUSSION

Mesothelia are essential for the generation of diverse cell types within all coelomic organs investigated thus far (Asahina et al., 2011; Eralp et al., 2005; Mikawa and Gourdie, 1996; Pérez-Pomares et al., 2004; Que et al., 2008; Wilm et al., 2005). Despite the importance of this cell type in organogenesis, the origin of mesothelium had only been established in the heart, where mesothelium is derived from a localized, extrinsic cell population: the PE. Identification of the origin of mesothelial cells is essential for studies of the molecular regulation of mesothelial differentiation, vascular formation, and mesothelial-dependent signaling in intestinal development and organogenesis in general. Here, using three independent methods, we demonstrate that intestinal mesothelium is derived from a resident population of cells broadly distributed within the splanchnic mesoderm. Thus, gut mesothelium does not arise in the same manner as described in the heart and reveals a novel paradigm for the generation of this essential cell type. Discovery of the origin of gut mesothelium is crucial for further analysis of regulatory mechanisms governing mesothelial development, repair in the adult and origin of disease.

Previously, we have demonstrated through a genetic lineage-tracing study in mouse that vascular smooth muscle cells of the intestine were derived from mesothelium. Furthermore, expression of *Wt1* was first observed in the mesentery and then progressively encompassed the intestinal tube, suggesting a migratory mesothelial population may exist, as observed in the heart (Wilm et al., 2005). However, a PE-like structure or clear evidence of a migratory population was not identified. Furthermore, *Wt1* is not a marker specific only to mesothelium (Zhou et al., 2011). Here, through the use of direct labeling and transplantation studies in the avian embryo, we have demonstrated that mesothelial progenitors of the intestine are broadly resident to the splanchnic mesoderm and not derived from an exogenous migratory source. This progenitor population is present prior to tube formation but does not specifically express *Wt1*. Although there may be variation

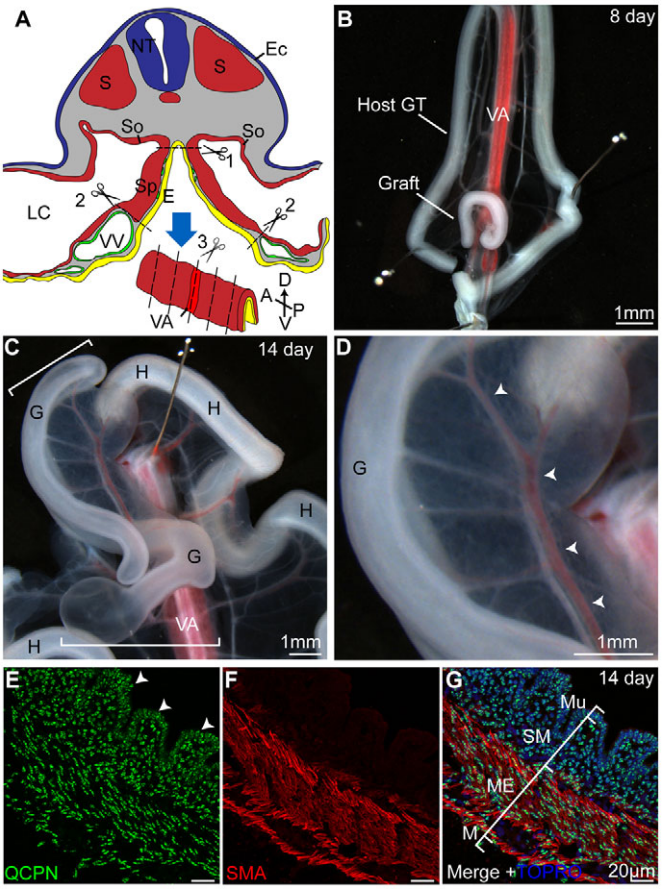

Fig. 7. Transplanted splanchnopleure forms a highly structured gut tube. (**A**) Transplants were generated by cutting along the dorsal aspect of the splanchnopleure (1) and the ventral edges near the vitelline veins (2). The splanchnopleure was then cut along the AP axis (3) to generate six or seven pieces for transplantation. (**B**) A representative graft-derived gut tube 8 days after transplantation. The graft had generated a tube and attached to the mesentery of the host gut tube. (**C**) A representative graft-derived gut tube 14 days after transplantation (G, bracketed). The graft-derived gut tube was attached to the host (H) via a mesentery. (**D**) The mesentery of the graft-derived gut tube contained a regular arrangement of blood vessels (arrowheads). (**E-G**) Sections through the graft-derived gut tube demonstrated normal morphogenesis with villi (arrowheads), submucosa (SM) and a SMA-positive muscularis externus layer. All layers were derived from quail cells (QCPN positive, green). E, endoderm; Ec, ectoderm; G, graft-derived gut tube; H, host gut tube; LC, lateral cavity; M, mesothelium; ME, muscularis externa; Mu, mucosa; NT, neural tube; S, somite; So, somatic mesoderm; Sp, splanchnic mesoderm; SM, submucosa; VA, vitelline artery; VV, vitelline vein.

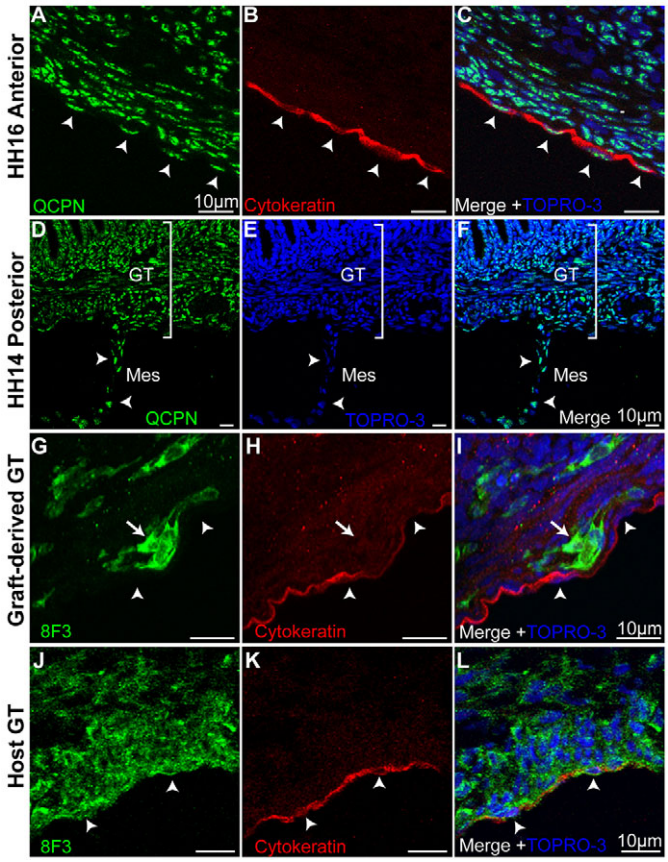

Fig. 8. Graft mesothelium is quail derived. (**A-C**) Section of graft-derived gut tube generated from tissue isolated from the anterior splanchnopleure of a HH16 quail donor. Co-staining for QCPN and cytokeratin demonstrated that the mesothelial cells lining the graft were quail derived (arrowheads). (**D-F**) Section of a graft-derived gut tube generated from the posterior splanchnopleure of a HH14 quail donor. QCPN staining demonstrates the mesenteric mesothelium is quail derived (arrowheads). (**G-I**) Host-derived cells (8F3-positive) were also identified within the graft (arrows). However, 8F3-positive chick cells were only rarely (6%) identified within the mesothelial layer (arrowheads) of the graft-derived gut tube. (**J-L**) Staining of a chick (host) gut tube reveals mesothelial cells (arrowheads) robustly label with the chick marker 8F3. GT, gut tube; Mes, mesentery.

between species in intestinal mesothelial origin and *Wt1* expression patterns, it is possible that murine mesothelial progenitors are also resident broadly in the intestine and *Wt1* is expressed in a dorsal-ventral direction as mesothelial differentiation proceeds. Further experimentation is needed to resolve this issue among different species.

The intestines, lungs, liver and pancreas are all gut tube derivatives formed from endoderm or endodermal buds that are surrounded by splanchnic mesoderm. By contrast, the heart wall is not a gut tube derivative but rather is derived solely from splanchnic mesoderm, excluding endoderm dorsally. The splanchnic mesoderm, which makes up the majority of the heart wall, is not thought to contain mesothelial progenitors (Gittenberger-de Groot et al., 2000; Männer et al., 2005). By contrast, the present study demonstrates that mesothelial precursors are resident broadly at the surface of the developing gut splanchnic mesoderm prior to endodermal budding and mucosal differentiation. Considering the unique features of cardiac development and the early specialization of the cardiac splanchnic mesoderm (i.e. it is a contractile tube before PE-derived mesothelium contacts the organ), we postulate mesothelial development in the lungs, liver and pancreas, as gut tube derivatives will be found to more closely resemble the intestinal rather than the cardiac model of mesothelial development.

The molecular foundation for the variation in proepicardial and intestinal mesothelial development is currently unknown. However, Ishii et al. report that the liver bud is at least partially responsible

for induction of markers of the PE, including *Wt1*, *Tbx18* and capsulin. Liver bud transplanted ectopically into the lateral embryo distal to the heart induced *Wt1* in the closely adjoining tissue. Interestingly, the lung bud and stomach did not have similar inductive capabilities in that system (Ishii et al., 2007). For the majority of the mesothelium not in contact with the liver bud, alternative inductive tissues and signals must be involved. Other studies have uncovered potential roles for BMP in villous protrusion of the PE (Ishii et al., 2010), a behavior observed in cardiac but not intestinal mesothelial development (from the current study), and for both BMP and FGF signals in the lineage specification of epicardial cells (Kruithof et al., 2006; Schlueter et al., 2006). With identification of the fundamental mechanism of intestinal mesothelial formation, studies on the molecular regulation of behaviors unique to either the intestinal or cardiac mesothelium can proceed.

Although the origin of mesothelial cells in the intestine and heart are clearly divergent, there do exist conserved features of mesothelial development and differentiation. The presence of a small number of host mesothelial cells in graft-derived gut tubes suggests that intestinal mesothelium can be migratory as previously observed with epicardial mesothelium. Whether this is a normally occurring event in gut development or simply a 'blending' of cells in this particular experimental model, it is evident that mesothelial progenitors of the gut and/or definitive gut mesothelium are capable of movement or active migration. Mesothelial cells in the heart, lungs, intestines and liver all give rise to stromal cells, including vascular smooth muscle, endothelium, fibroblasts and other 'mesenchymal' cells (Asahina et al., 2011; Dettman et al., 1998; Eralp et al., 2005; Mikawa and Gourdie, 1996; Pérez-Pomares et al., 2004; Que et al., 2008; Wilm et al., 2005). Both cardiac and peritoneal mesothelia of the adult retain the ability to generate stromal progeny. When stimulated, adult omental mesothelial cells differentiate into vascular smooth muscle cells and can directly contribute cells to an injured blood vessel (Kawaguchi et al., 2007; Shelton et al., 2012). Fibroblast and vascular smooth muscle cell differentiation from previously quiescent mesothelium has also been observed following myocardial infarction (Zhou and Pu, 2011). Thus, although the mechanism generating intestinal mesothelial cells is different from that of the heart, once established, these two progenitor populations appear to have similar differentiative potentials.

Other disease processes involving mesothelia reflect the developmental potential of this cell type. For example, peritoneal sclerosis, a fibrotic thickening of the abdominal serosal membranes, is frequently observed following peritoneal dialysis (Devuyst et al., 2010). Mesothelial cells have recently been recognized both as a source of fibrotic cells and a signaling center for aberrant vasculogenesis (Aroeira et al., 2005; Braun et al., 2011; Yáñez-Mó et al., 2003; Yung and Chan, 2009). In another example, pulmonary fibrosis is first observed as a fibrotic thickening just below the pulmonary mesothelium that progressively moves inwards (King et al., 2011). The role of mesothelium in this disease has also recently been the focus of studies and reviews as a signaling center or source of fibrotic cells (Acencio et al., 2007; Decologne et al., 2007; Mutsaers et al., 2004). These pathologies have a direct root in the developmental potential of mesothelium to give rise to fibroblasts and vascular smooth muscle. Thus, investigation of the diversity of mesothelial populations is crucial to understanding their behavior in these various organs systems and disease processes.

Following discovery of the pro-epicardium, studies on development of cardiac mesothelium were able to rapidly progress. Currently, our understanding of epicardial biology encompasses the detailed cell lineage, mechanisms of molecular differentiation during development and pathological behavior. We are now poised to move forward with similar studies of non-cardiac mesothelial populations. Mesothelial cells of diverse organs and body cavities have been considered a uniform population owing to their ultrastructural similarity and apparent shared developmental potential. Our data demonstrate that at least cardiac and intestinal mesothelia are heterogeneous populations with varied developmental histories that must be considered independently. Understanding the developmental origin of diverse mesothelia is essential for understanding the role mesothelial, vascular and stromal cells may play in the development and homeostasis of these organs in the adult.

Acknowledgements
Imaging was performed in part through the use of the VUMC Cell Imaging Shared Resource supported by National Institutes of Health (CA68485, DK20593, DK58404, HD15052, DK59637 and EY08126). Monoclonal antibodies were obtained from the Developmental Studies Hybridoma Bank developed under the auspices of the NICHD and maintained by The University of Iowa, Department of Biology, Iowa City, IA 52242, USA. We gratefully acknowledge Dr Jeanette Hyer (UCSF) for providing the pSNID-GFP retrovirus and training on its use; Dr Michael Stark (BYU) for providing the pCIG-GFP construct; and Dr Connie Cepko (Harvard) for providing the pCAGGS construct.

Funding
The authors' research was funded by an American Heart Association pre-doctoral fellowship [09PRE2060828] and by a National Institutes of Health grant [R01 DK83234]. Deposited in PMC or release after 12 months.

Competing interests statement
The authors declare no competing financial interests.

Supplementary material
Supplementary material available online at
http://dev.biologists.org/lookup/suppl/doi:10.1242/dev.082396/-/DC1

References

Acencio, M. M., Vargas, F. S., Marchi, E., Carnevale, G. G., Teixeira, L. R., Antonangelo, L. and Broaddus, V. C. (2007). Pleural mesothelial cells mediate inflammatory and profibrotic responses in talc-induced pleurodesis. *Lung* **185**, 343-348.

Aroeira, L. S., Aguilera, A., Selgas, R., Ramírez-Huesca, M., Pérez-Lozano, M. L., Cirugeda, A., Bajo, M. A., del Peso, G., Sánchez-Tomero, J. A., Jiménez-Heffernan, J. A. et al. (2005). Mesenchymal conversion of mesothelial cells as a mechanism responsible for high solute transport rate in peritoneal dialysis: role of vascular endothelial growth factor. *Am. J. Kidney Dis.* **46**, 938-948.

Asahina, K., Zhou, B., Pu, W. T. and Tsukamoto, H. (2011). Septum transversum-derived mesothelium gives rise to hepatic stellate cells and perivascular mesenchymal cells in developing mouse liver. *Hepatology* **53**, 983-995.

Braun, N., Alscher, D. M., Fritz, P., Edenhofer, I., Kimmel, M., Gaspert, A., Reimold, F., Bode-Lesniewska, B., Ziegler, U., Biegger, D. et al. (2011). Podoplanin-positive cells are a hallmark of encapsulating peritoneal sclerosis. *Nephrol. Dial. Transplant.* **26**, 1033-1041.

Chegini, N. (2008). TGF-beta system: the principal profibrotic mediator of peritoneal adhesion formation. *Semin. Reprod. Med.* **26**, 298-312.

Decologne, N., Kolb, M., Margetts, P. J., Menetrier, F., Artur, Y., Garrido, C., Gauldie, J., Camus, P. and Bonniaud, P. (2007). TGF-beta1 induces progressive pleural scarring and subpleural fibrosis. *J. Immunol.* **179**, 6043-6051.

Dettman, R. W., Denetclaw, W., Jr, Ordahl, C. P. and Bristow, J. (1998). Common epicardial origin of coronary vascular smooth muscle, perivascular fibroblasts, and intermyocardial fibroblasts in the avian heart. *Dev. Biol.* **193**, 169-181.

Devuyst, O., Margetts, P. J. and Topley, N. (2010). The pathophysiology of the peritoneal membrane. *J. Am. Soc. Nephrol.* **21**, 1077-1085.

Eralp, I., Lie-Venema, H., DeRuiter, M. C., van den Akker, N. M., Bogers, A. J., Mentink, M. M., Poelmann, R. E. and Gittenberger-de Groot, A. C. (2005). Coronary artery and orifice development is associated with proper

timing of epicardial outgrowth and correlated Fas-ligand-associated apoptosis patterns. *Circ. Res.* **96**, 526-534.
Gittenberger-de Groot, A. C., Vrancken Peeters, M. P., Bergwerff, M., Mentink, M. M. and Poelmann, R. E. (2000). Epicardial outgrowth inhibition leads to compensatory mesothelial outflow tract collar and abnormal cardiac septation and coronary formation. *Circ. Res.* **87**, 969-971.
Hamburger, V. and Hamilton, H. L. (1992). A series of normal stages in the development of the chick embryo. 1951. *Dev. Dyn.* **195**, 231-272.
Ho, E. and Shimada, Y. (1978). Formation of the epicardium studied with the scanning electron microscope. *Dev. Biol.* **66**, 579-585.
Ishii, Y., Langberg, J. D., Hurtado, R., Lee, S. and Mikawa, T. (2007). Induction of proepicardial marker gene expression by the liver bud. *Development* **134**, 3627-3637.
Ishii, Y., Garriock, R. J., Navetta, A. M., Coughlin, L. E. and Mikawa, T. (2010). BMP signals promote proepicardial protrusion necessary for recruitment of coronary vessel and epicardial progenitors to the heart. *Dev. Cell* **19**, 307-316.
Kawaguchi, M., Bader, D. M. and Wilm, B. (2007). Serosal mesothelium retains vasculogenic potential. *Dev. Dyn.* **236**, 2973-2979.
King, T. E., Jr, Pardo, A. and Selman, M. (2011). Idiopathic pulmonary fibrosis. *Lancet* **378**, 1949-1961.
Kruithof, B. P., van Wijk, B., Somi, S., Kruithof-de Julio, M., Pérez Pomares, J. M., Weesie, F., Wessels, A., Moorman, A. F. and van den Hoff, M. J. (2006). BMP and FGF regulate the differentiation of multipotential pericardial mesoderm into the myocardial or epicardial lineage. *Dev. Biol.* **295**, 507-522.
Lassiter, R. N., Dude, C. M., Reynolds, S. B., Winters, N. I., Baker, C. V. and Stark, M. R. (2007). Canonical Wnt signaling is required for ophthalmic trigeminal placode cell fate determination and maintenance. *Dev. Biol.* **308**, 392-406.
Manasek, F. J. (1969). Embryonic development of the heart. II. Formation of the epicardium. *J. Embryol. Exp. Morphol.* **22**, 333-348.
Männer, J., Schlueter, J. and Brand, T. (2005). Experimental analyses of the function of the proepicardium using a new microsurgical procedure to induce loss-of-proepicardial-function in chick embryos. *Dev. Dyn.* **233**, 1454-1463.
McGlinn, E. and Mansfield, J. H. (2011). Detection of gene expression in mouse embryos and tissue sections. *Methods Mol. Biol.* **770**, 259-292.
Mikawa, T. and Gourdie, R. G. (1996). Pericardial mesoderm generates a population of coronary smooth muscle cells migrating into the heart along with ingrowth of the epicardial organ. *Dev. Biol.* **174**, 221-232.
Minot, C.-S. (1890). The mesoderm and the coelom of vertebrates. *Am. Nat.* **24**, 877-898.
Moore, K. L. and Persaud, T. V. N. (1998). *The Developing Human: Clinically Oriented Embryology*. Philadelphia: Saunders.
Morimoto, M., Liu, Z., Cheng, H. T., Winters, N., Bader, D. and Kopan, R. (2010). Canonical Notch signaling in the developing lung is required for determination of arterial smooth muscle cells and selection of Clara versus ciliated cell fate. *J. Cell Sci.* **123**, 213-224.
Mutsaers, S. E. (2002). Mesothelial cells: their structure, function and role in serosal repair. *Respirology* **7**, 171-191.
Mutsaers, S. E. and Wilkosz, S. (2007). Structure and function of mesothelial cells. *Cancer Treat. Res.* **134**, 1-19.
Mutsaers, S. E., Prele, C. M., Brody, A. R. and Idell, S. (2004). Pathogenesis of pleural fibrosis. *Respirology* **9**, 428-440.
Osler, M. E. and Bader, D. M. (2004). Bves expression during avian embryogenesis. *Dev. Dyn.* **229**, 658-667.
Pérez-Pomares, J. M., Carmona, R., González-Iriarte, M., Macías, D., Guadix, J. A. and Muñoz-Chápuli, R. (2004). Contribution of mesothelium-derived cells to liver sinusoids in avian embryos. *Dev. Dyn.* **229**, 465-474.
Que, J., Wilm, B., Hasegawa, H., Wang, F., Bader, D. and Hogan, B. L. (2008). Mesothelium contributes to vascular smooth muscle and mesenchyme during lung development. *Proc. Natl. Acad. Sci. USA* **105**, 16626-16630.
Schlueter, J., Männer, J. and Brand, T. (2006). BMP is an important regulator of proepicardial identity in the chick embryo. *Dev. Biol.* **295**, 546-558.
Schulte, I., Schlueter, J., Abu-Issa, R., Brand, T. and Männer, J. (2007). Morphological and molecular left-right asymmetries in the development of the proepicardium: a comparative analysis on mouse and chick embryos. *Dev. Dyn.* **236**, 684-695.
Shelton, E. L., Poole, S. D., Reese, J. and Bader, D. M. (2012). Omental grafting: a cell-based therapy for blood vessel repair. *J. Tissue Eng. Regen. Med.* doi: 10.1002/term.528.
Takaba, K., Jiang, C., Nemoto, S., Saji, Y., Ikeda, T., Urayama, S., Azuma, T., Hokugo, A., Tsutsumi, S., Tabata, Y. et al. (2006). A combination of omental flap and growth factor therapy induces arteriogenesis and increases myocardial perfusion in chronic myocardial ischemia: evolving concept of biologic coronary artery bypass grafting. *J. Thorac. Cardiovasc. Surg.* **132**, 891-899.
Venters, S. J., Dias da Silva, M. R. and Hyer, J. (2008). Murine retroviruses re-engineered for lineage tracing and expression of toxic genes in the developing chick embryo. *Dev. Dyn.* **237**, 3260-3269.
Wilm, B., Ipenberg, A., Hastie, N. D., Burch, J. B. and Bader, D. M. (2005). The serosal mesothelium is a major source of smooth muscle cells of the gut vasculature. *Development* **132**, 5317-5328.
Wu, M., Smith, C. L., Hall, J. A., Lee, I., Luby-Phelps, K. and Tallquist, M. D. (2010). Epicardial spindle orientation controls cell entry into the myocardium. *Dev. Cell* **19**, 114-125.
Yáñez-Mó, M., Lara-Pezzi, E., Selgas, R., Ramírez-Huesca, M., Domínguez-Jiménez, C., Jiménez-Heffernan, J. A., Aguilera, A., Sánchez-Tomero, J. A., Bajo, M. A., Alvarez, V. et al. (2003). Peritoneal dialysis and epithelial-to-mesenchymal transition of mesothelial cells. *N. Engl. J. Med.* **348**, 403-413.
Yung, S. and Chan, T. M. (2009). Intrinsic cells: mesothelial cells – central players in regulating inflammation and resolution. *Perit. Dial. Int.* **29 Suppl. 2**, S21-S27.
Zhang, Q. X., Magovern, C. J., Mack, C. A., Budenbender, K. T., Ko, W. and Rosengart, T. K. (1997). Vascular endothelial growth factor is the major angiogenic factor in omentum: mechanism of the omentum-mediated angiogenesis. *J. Surg. Res.* **67**, 147-154.
Zhou, B. and Pu, W. T. (2011). Epicardial epithelial-to-mesenchymal transition in injured heart. *J. Cell. Mol. Med.* **15**, 2781-2783.
Zhou, B., Honor, L. B., He, H., Ma, Q., Oh, J. H., Butterfield, C., Lin, R. Z., Melero-Martin, J. M., Dolmatova, E., Duffy, H. S. et al. (2011). Adult mouse epicardium modulates myocardial injury by secreting paracrine factors. *J. Clin. Invest.* **121**, 1894-1904.